Temperature and pH dependence of the deprotonation step L550 .fwdarw. M412 in the bacteriorhodopsin photocycle

ARTICLE *in* THE JOURNAL OF PHYSICAL CHEMISTRY · DECEMBER 1991

Impact Factor: 2.78 · DOI: 10.1021/j100178a035

3 AUTHORS, INCLUDING:

Mostafa A El-Sayed
Georgia Institute of Technology
676 PUBLICATIONS **54,961** CITATIONS

SEE PROFILE

straightforward application of the Slater rules[37] yield

$$N_c^2 = \{4! \times 2[1 - \langle H|B\rangle^2 + \langle H|A\rangle^2 - \langle A|B\rangle^2 - 2\langle H|A\rangle\langle H|B\rangle\langle A|B\rangle + \langle H|B\rangle^2\langle A|B\rangle^2]\}^{-1} \quad (B.5)$$

and a similar expression is obtained for N_i^2. The overlap $\langle\psi_c|\psi_i\rangle$ is

$$\langle\psi_c|\psi_i\rangle = N_c N_i[\langle D_1|D_3\rangle + \langle D_2|D_4\rangle - \langle D_2|D_3\rangle - \langle D_1|D_4\rangle] \quad (B.6)$$

with

$$\langle D_1|D_3\rangle = \langle D_2|D_4\rangle = 4!\{\langle H|A\rangle\langle H|B\rangle - \langle H|B\rangle^2\langle A|B\rangle - \langle H|A\rangle^2\langle A|B\rangle + \langle H|A\rangle\langle H|B\rangle\langle A|B\rangle^2\}$$

$$\langle D_1|D_4\rangle = \langle D_2|D_3\rangle = 4!\{-\langle H|A\rangle\langle H|B\rangle + \langle A|B\rangle + \langle A|B\rangle^2\langle H|A\rangle\langle H|B\rangle - \langle A|B\rangle^3\} \quad (B.7)$$

Combination of the above expressions with the weak overlap approximation adopted by Coulson and Danielsson,[25] i.e., $\langle A|B\rangle \approx 0$, yields

$$\langle\psi_c|\psi_i\rangle = \left[\frac{2}{1 - \langle H|B\rangle^2 + \langle H|A\rangle^2}\right]^{1/2}\left[\frac{2}{1 - \langle H|A\rangle^2 + \langle H|B\rangle^2}\right]^{1/2} \times \langle H|A\rangle\langle H|B\rangle \quad (B.8)$$

in agreement with previous work.[25]

We have tested numerically the overlap neglect approximation for O–H···N at R = 2.8, 2.9, 3.0, and 3.1 Å and different positions of H. In this particular case, the Slater atomic orbitals characterized by the appropriate effective nuclear charges are $A \equiv 2p_O$, $H \equiv 1s_H$, and $B \equiv 2p_N$. The numerical values for the integrals over AO at several internuclear separations have been taken directly or interpolated from standard tables.[61] The overlap integral $\langle 2p_O|2p_N\rangle$ is typically at least 1 order of magnitude smaller than $\langle 1s_H|2p_O\rangle$ and $\langle 1s_H|2p_N\rangle$ and it is justifiably neglected in the expansion for $\langle\psi_c|\psi_i\rangle$. We also find that as $\langle 1s_H|2p_O\rangle$ increases, $\langle 1s_H|2p_N\rangle$ decreases in such a way that their product remains constant over a range of r values near 1 Å. Thus this product contribution to the overlap is essentially constant with r.

If we proceed analogously with $\langle\psi_p|\psi_i\rangle$, the overlap between the states ψ_n and ψ_i can be computed for different R and r values. This overlap is also approximately constant with respect to r at small R (if we assume ψ_n to be a mixture of 20% the polar state and 80% the covalent state, namely, $k_c = 0.894$ and $k_p = 0.447$). As R increases, an increase in r renders the hydrogen-bonded complex ionic, in which form the polar state ψ_p has a negligible contribution, i.e., $k_p \to 0$, and consequently S is also approximately constant with r.

(61) Mulliken, R. S.; Rieke, C. A.; Orloff, D.; Orloff, H. *J. Chem. Phys.* **1949**, *17*, 1248.

Temperature and pH Dependence of the Deprotonation Step $L_{550} \rightarrow M_{412}$ in the Bacteriorhodopsin Photocycle

Gloria C. Lin, E. S. Awad, and M. A. El-Sayed*

Department of Chemistry and Biochemistry, University of California at Los Angeles, 405 Hilgard Avenue, Los Angeles, California 90024 *(Received: April 11, 1991)*

The deprotonation step $L_{550} \rightarrow M_{412}$ in the photocycle of bacteriorhodopsin (bR) exhibits biphasic kinetics consistent with rate constants k_{fast} and k_{slow} which differ by an order of magnitude. The kinetics of the slow formation of M_{412} monitored at 405 nm were investigated as a function of temperature and pH, in the range 10–25 °C and pH 3–12. Two proposals have been made previously to account for the presence of the biexponential kinetics of M_{412} formation. One proposal attributed the existence of the two kinetic components to the presence of two species of bR, which react along parallel pathways (i.e., heterogeneity). The second proposal explained the kinetics by a mechanism involving forward and reverse reactions which are pH dependent. We have selected the first mechanism to discuss our pH and temperature results. The values of k_{slow} (which are correlated with the rates of the proton pumping) are found to be independent of pH in the range pH 3–7 but increase continuously above pH 8 to a value 8-fold larger at pH 12, implying that at pH 3–7 $\Delta H^{\ddagger}$ and $T\Delta S^{\ddagger}$ offset each other but at pH ≥8 the entropic effect increases with pH faster than the enthalpic effect. The pH profile of the relative amplitudes, C_{fast} and C_{slow}, shows that there is a transition at pH 8–10, which is controlled by a single prototropic group with apparent pK 9.0. The activation parameters $\Delta H^{\ddagger}$ and $\Delta S^{\ddagger}$ corresponding to k_{slow} were determined over the range pH 3–12. While the value of k_{slow} does not show sudden changes at any pH, a sharp discontinuity was observed in each of the activation parameters at pH 10–11. This might suggest a helix–coil transition in the active site environment. The sharpness of the transition could be ascribed to a simultaneous attack by hydroxide ions on four prototropic groups with an average pK 10.5. The inversion of sign in the activation entropy $\Delta S^{\ddagger}$ (+93 J K^{-1} mol^{-1} at pH 10 to −39 J K^{-1} mol^{-1} at pH 11) might suggest that below pH 10 the proton translocation sequence involves considerable structuring in the reactant L_{550} which becomes loosened in the transition-state $L^{\ddagger}$, whereas above pH 11 the reactant L_{550} is partially random coil conformation, which is less structured than the transition-state $L^{\ddagger}$, thereby allowing additional access to hydroxide ions and solvent water to participate in the proton translocation.

Introduction

The purple membrane (pm) in *Halobacterium halobium* contains a single protein, bacteriorhodopsin (bR), the function of which is to translocate hydrogen ions from the cytoplasmic side of the membrane to a highly saline medium outside the bacterial cell.[1-12] The energy to create the gradient in the chemical potential of H^+ is derived from the absorption of light at 568 nm.

(1) Oesterhelt, D.; Stoeckenius, W. *Nature (London) New Biol.* **1971**, *233*, 149.

0022-3654/91/2095-10442$02.50/0

This excitation energy, which per photon absorbed corresponds to 211 kJ mol^{-1}, takes the bR molecule around a cycle consisting of steps that occur on time scales ranging from femtoseconds to milliseconds:[9,13-20]

$$bR_{568} \xrightarrow{h\nu} bR^* \xrightarrow[200\ fs]{} I_{460} \xrightarrow[400\ fs]{} J_{625} \xrightarrow[5\ ps]{} K_{610} \xrightarrow[2\ \mu s]{}$$
$$L_{550} \xrightarrow[60\ \mu s]{-H^+} M_{412} \xrightarrow[(ms)]{+H^+} N_{520} \rightarrow O_{640} \rightarrow bR_{568}$$

The chromophore, retinal, is attached through a protonated Schiff base (PSB) linkage to Lys-216 in the G-helix of bR.[3,4,9,12,21-23]

The process of proton translocation is coupled to the photocycle at the point in which deprotonation of the PSB converts L to M, followed by the decay of M as a consequence of the reprotonation of the Schiff base

$$L_{550}(\sim NH) + B_1 \rightarrow M_{412}(\sim N:) + HB_1$$

$$M_{412}(\sim N:) + HB_2 \rightarrow N_{520}(\sim NH) + B_2$$

where HB_1,B_1 and HB_2,B_2 are Brønsted acid-base pairs which are located in the environment of the retinylidene. The hydroxyl group of Tyr and the carboxyl group of Asp have been implicated.[24-30] The recent model for the structure of bR,[12] using the results of the pumping efficiencies of singly substituted bR mutants[28-33] and other FTIR results,[34,35] suggests that aspartate-85 (or -212) is the proton acceptor while aspartic acid 96 is the proton donor. It may well be that other amino acid side groups act sequentially, or in a concerted manner, as acid-base intermediates in the transduction of H^+, constituting a proton wire which operates as a concerted mechanism, or by participating in a rapid sequence of discrete proton transfer steps from one group to another.[36,37] At the extremes of the translocation sequence one proton is accepted from H_3O^+ at the cytoplasmic side of the purple membrane and one proton is transferred to a water molecule or hydroxide ion at the periplasmic side of the membrane. It is to be noted that M is the only intermediate in the photocycle in which the Schiff base is unprotonated.

Kinetic measurements in several laboratories have shown that when the formation of the M_{412} intermediate is monitored at 405 nm, the progress curves are biphasic, with rate constants differing by an order of magnitude.[24,38-44] Furthermore, the M decay kinetics, when monitored at 405 nm, are also biphasic.[42-49] In addition, there appears to be a species R_{350} whose formation and decay occur parallel to the M kinetics, when the photocycle operates in a highly saline medium of about 4 M NaCl.[49] It has been suggested that the species N_{520},[16,19,50] L',[34] P,[51] and R_{350}[49] are the same as N_{550}.[20]

The origin of the biphasic nature of the kinetics is not quite understood at the moment. Hanamoto et al.[24] suggested that the two components result from protein heterogeneity due to an acid-base equilibrium of an amino acid near the PSB with pK_a $\sim$ 9.5. The PSB located near the undissociated amino acid is expected to have a different environment from the PSB located near the ionized form. This gives rise to a difference in the rate of the protein conformation change within the active site which determines the rate of the deprotonation process.[24] This type of heterogeneity was suggested by Raman spectroscopy[40] and other optical pH dependence studies.[45,49] More recently, the pH data were computer fitted well to a model that involves the N $\rightarrow$ M $\rightarrow$ L reverse reactions with rates that are pH dependent.[20,42-44] At the present, it is difficult to decide between the two mechanisms. In this paper, we shall use the model with two species of bR to discuss our pH and temperature dependence results with the focus on the slow component of bR deprotonation.

Experimental Section

Bacteriorhodopsin. Master slants of *H. halobium* ET1-001 strain were kindly supplied to us by Professor R. Bogomolni and Professor W. Stoeckenius. Purple membrane was isolated by a

(2) Oesterhelt, D.; Stoeckenius, W. *Proc. Natl. Acad. Sci. U.S.A.* **1973**, *70*, 2853.
(3) Khorana, H. G.; Gerber, G. E.; Herhily, W. C.; Gray, C. P.; Anderegg, R. J.; Nihei, K.; Biemann, K. *Proc. Natl. Acad. Sci. U.S.A.* **1979**, *76*, 5046.
(4) Ovchinnikov, Y. A.; Abdulaev, N. G.; Feignia, M. Y.; Kisalev, A. V.; Lobanov, N. A. *FEBS Lett.* **1979**, *100*, 219.
(5) Stoeckenius, W.; Lozier, R. H.; Bogomolni, R. A. *Biochim. Biophys. Acta* **1979**, *505*, 215.
(6) Stoeckenius, W.; Bogomolni, R. A. *Annu. Rev. Biochem.* **1982**, *52*, 587.
(7) Lanyi, J. K. In *Bioenergetics (New Comprehensive Biochemistry*; Ernster, L., Ed.; Elsevier/North Holland: Amsterdam, 1984; Vol. 9, p 315.
(8) Ovchinnikov, Y. A. *Chem. Scr.* **1987**, *27B*, 149.
(9) Khorana, H. G. *J. Biol. Chem.* **1988**, *263*, 7439.
(10) Malmström, B. G. *FEBS Lett.* **1989**, *250*, 9.
(11) Trissl, H. W. *Photochem. Photobiol.* **1990**, *51*, 793.
(12) Henderson, R.; Baldwin, J. M.; Ceska, T. A.; Zemlin, F.; Beckmann, E.; Downing, K. H. *J. Mol. Biol.* **1990**, *213*, 899.
(13) Lewis, A.; Spoonhower, J.; Bogomolni, R. A.; Lozier, R. H.; Stoeckenius, W. *Proc. Natl. Acad. Sci. U.S.A.* **1974**, *71*, 4462.
(14) Lozier, R. H.; Bogomolni, R. A.; Stoeckenius, W. *Biophys. J.* **1975**, *15*, 955.
(15) Marcus, M. A.; Lewis, A. *Science* **1977**, *195*, 1328.
(16) Braiman, M.; Mathies, R. *Proc. Natl. Acad. Sci. U.S.A.* **1982**, *79*, 403.
(17) Fodor, S. P.; Ames, J. B.; Gebhard, R.; van den Berg, E. M. M.; Stoeckenius, W.; Lugtenburg, J.; Mathies, R. A. *Biochemistry* **1988**, *27*, 7097.
(18) Mathies, R. A.; Brito Cruz, C. H.; Pollard, W. T.; Shank, C. V. *Science* **1988**, *240*, 777.
(19) Pollard, W. T.; Brito Cruz, C. H.; Shank, C. V.; Mathies, R. A. *J. Chem. Phys.* **1989**, *90*, 199.
(20) Ames, J. B.; Mathies, R. A. *Biochemistry* **1990**, *29*, 7181.
(21) Bridgen, J.; Walker, I. *Biochemistry* **1976**, *15*, 792.
(22) Katre, N. V.; Wolber, P. K.; Stoeckenius, W.; Stroud, R. M. *Proc. Natl. Acad. Sci. U.S.A.* **1981**, *78*, 4068.
(23) Heyn, M. P.; Braun, D.; Dencher, N. A.; Fahr, A.; Holz, M.; Lindau, M.; Seiff, F.; Wallat, I.; Westerhausen, J. *Ber. Bunsenges. Phys. Chem.* **1988**, *92*, 1045.
(24) Hanamoto, J. H.; Dupuis, J. P.; El-Sayed, M. A. *Proc. Natl. Acad. Sci. U.S.A.* **1984**, *81*, 7083.
(25) Bogomolni, R. A.; Stubbs, L.; Lany, J. K. *Biochemistry* **1978**, *17*, 1037.
(26) Hess, B.; Kuschmitz, D. *FEBS Lett.* **1979**, *100*, 334.
(27) Roepe, P.; Scherrer, P.; Ahl, P. L.; Das Gupta, S. K.; Bogomolni, R. A.; Herzfeld, J.; Rothschild, K. J. *Biochemistry* **1987**, *26*, 6708.
(28) Butt, H. J.; Fendler, F.; Bamberg, E.; Tittor, J.; Oesterhelt, D. *EMBO J.* **1989**, *8*, 1657.
(29) Tittor, J.; Soell, C.; Oesterhelt, D.; Butt, H. J.; Bamberg, E. *EMBO J.* **1989**, *8*, 3477.
(30) Gerwert, K.; Hess, B.; Soppa, J.; Oesterhelt, D. *Proc. Natl. Acad. Sci. U.S.A.* **1989**, *86*, 4943.
(31) Marinetti, T.; Subramnaiam, S.; Mogi, T.; Marti, T.; Khorana, H. G. *Proc. Natl. Acad. Sci. U.S.A.* **1989**, *86*, 529.
(32) Otto, H.; Marti, T.; Holz, M.; Moti, T.; Stern, L. J.; Engel, F.; Khorana, H. G.; Heyn, M. *Proc. Natl. Acad. U.S.A.* **1990**, *87*, 1018.
(33) Otto, H.; Marti, T.; Holz, M.; Mogi, T.; Stern, L. J.; Engel, F.; Khorana, H. G.; Heyn, M. P. *Proc. Natl. Acad. Sci. U.S.A.* **1990**, *86*, 9228.
(34) Siebert, F.; Mantele, W.; Kreutz, W. *FEBS Lett.* **1982**, *141*, 82.
(35) Braiman, M. S.; Mogi, T.; Marti, T.; Stern, L. J.; Khorana, H. G.; Rothschild, K. J. *Biochemistry* **1988**, *27*, 8516.
(36) Nagle, J. F.; Morowitz, H. J. *Proc. Natl. Acad. Sci. U.S.A.* **1978**, *15*, 298.
(37) Papadopoulos, G.; Dencher, N. A.; Zaccai, G.; Buldt, G. *J. Mol. Biol.* **1990**, *214*, 15.
(38) Fukumoto, J. M.; Hanamoto, J. H.; El-Sayed, M. A. 1984. *Photochem. Photobiol.* **1984**, *39*, 75.
(39) Dupuis, P.; El-Sayed, M. A. *Can. J. Chem.* **1985**, *63*, 1699.
(40) Diller, R.; Stockburger, M. *Biochemistry* **1988**, *27*, 7641.
(41) Bitting, H. C.; Jang, D. J.; El-Sayed, M. A. *Photochem. Photobiol.* **1990**, *52*, 593.
(42) Varo, G.; Lanyi, J. K. *Biochemistry* **1990**, *29*, 2241.
(43) Varo, G.; Duschl, A.; Lanyi, J. K. *Biochemistry* **1990**, *29*, 3798.
(44) Varo, G.; Lanyi, K. J. *Biochemistry* **1990**, *29*, 6858.
(45) Dancshazy, Z.; Govindjee, R.; Ebrey, T. G. *Proc. Natl. Acad. Sci. U.S.A.* **1988**, *85*, 6358.
(46) Nakagawa, M.; Ogura, T.; Maeda, A.; Kitagawa, T. *Biochemistry* **1989**, *28*, 1347.
(47) Eisenbach, M.; Bakker, E. P.; Korenstein, R.; Caplan, S. R. *FEBS Lett.* **1976**, *71*, 228.
(48) Kouyama, T.; Nasuda-Kouyama, A.; Ikegami, A.; Mathew, M. K.; Stoeckenius, W. *Biochemistry* **1988**, *27*, 5855.
(49) Dancshazy, Z.; Govindjee, R.; Nelson, B.; Ebrey, T. G. *FEBS Lett.* **1986**, *209*, 44.
(50) Braiman, M.; Mathies, R. *Biochemistry* **1980**, *19*, 5421.
(51) Drachev, L. A.; Kaulen, A. D.; Skulachev, V. P.; Zorina, V. V. *FEBS Lett.* **1986**, *209*, 316.

combination of procedures.[52,53]

Buffer and Sample Preparations. To cover the range pH 3–12, different buffer species with overlapping buffer capacity ranges were selected. The following were purchased from Sigma (St. Louis, MO): potassium dihydrogen phosphate (KH_2PO_4, pK_a = 7.2); tris(hydroxymethyl)aminomethane (Tris, pK_a = 8.3); 3-[(1,1-dimethyl-2-hydroxyethyl)amino]-2-hydroxypropanesulfonic acid (AMPSO, pK_a = 9.0); 2-amino-2-methyl-1-propanol (AMP, pK_a = 9.7); 3-(cyclohexylamino)-1-propanesulfonic acid (CAPS, pK_a = 10.4); potassium monohydrogen phosphate (K_2HPO_4, pK_a = 12.4). Stock solutions of buffers were 0.01 M in buffer species and 0.1 M in NaCl, the latter to maintain constant ionic strength in all samples. Buffers of desired pH were prepared by adding 2.0 M NaOH or 2.0 M HCl in amounts of a few submicroliters at a time. In the preparation of samples, one part of concentrated bR suspension (~5 OD) was combined with nine parts of buffer of desired pH in a 1 cm path length polystyrene cuvette so that the concentration of bR was the same in all samples.

Kinetic Measurements. The procedure followed for obtaining transient absorption at 405 nm was essentially the same as previously described.[24] Each sample was freshly prepared just before the kinetic run, and the pH and temperature were checked immediately before and after the data acquisition. A digital pH-meter was used (Beckman Φ71, Fullerton, CA). Temperature was regulated by circulating water from a constant-temperature bath (NESLAB RTE100D, Dublin, CA) and measured in the cuvette near the photolyzing region with a digital thermometer (Fisher Scientific NBS LCD) using a 3-mm probe (YSI 402). The bR photocycle was initiated by a 580-nm pulse from an N_2-pumped dye laser (Photochemical Research Associates LN 1000 and LN 102, Oak Ridge, TN). To allow sufficient time for bR_{568} recovery, especially at high pH, the laser was fired at a repetition rate of 0.5 Hz for runs at lower temperatures (10–15 °C) and 1.0 Hz at higher temperatures (20–25 °C). The laser pulse had an energy of 50 μJ with temporal pulse width of 0.5 ns and was collimated to a 2-mm spot size. The probe light from a 100-W Hg arc lamp (Pek Labs 401, Sunnyvale, CA) was passed through filters to isolate the 405-nm line, focused onto the sample, and monitored by a photomultiplier (RCA 1P28A, Lancaster, PA). A transient digitizer waveform recorder (Biomation 8100, Santa Clara, CA) interfaced with a personal computer (Relisys PC-Craft, Milpitas, CA) was used to obtain the transient signal and kinetic constants. For each data acquisition, the rise of absorption at 405 nm was averaged over 1000 shots. Runs at a given temperature and pH were performed at least twice.

Results and Discussion

1. Biexponential Kinetics. As we indicated under Introduction, there are at present two different mechanisms explaining the biphasic kinetics of the M_{412} formation in the bR photocycle. In the recent mechanism[20,42–44] the two components result from pH-dependent reverse reactions. The support for this mechanism is the ability to computer fit the pH-dependent results. The alternate mechanism[24,40,41,45] assumes the presence of two parallel photocycles corresponding to k_{fast} and k_{slow}, resulting from different forms of bR_{568} in dynamic equilibrium and controlled by pH, ionic strength, and temperature. It was proposed that the equilibrium between these forms involves an acid–base equilibrium[24] with a pK_a value near 9 in the native bR_{568} ground state, depending on the ionic strength. In this picture of the active site one form of bR has the undissociated form of the acid(s), while in the other has the ionized form(s). Hanamoto et al.[24] proposed originally that the acid involved might be tyrosine, as it was understood at the time that the new absorption appearing at 296 nm during the M_{412} formation was assigned to tyrosinate.[26,28] The pK_a of the absorption near 296 nm had a value higher than 9. Since recent NMR[54,55] and Raman[40] results conclude that tyrosinate is not observed during the photocycle, one is forced to find another candidate for the acid having pK_a near 9. It was previously suggested[56] that the absorption near 296 nm might result from the charge perturbation of a tryptophan residue, giving an apparent pK_a near 9. The fact that some of the aspartic acids in bR are found with pK_a near this value[34] makes aspartic acid a possible candidate for creating the heterogeneity responsible for the different types of bR present.

There are some observations that lend strong support to the presence of different types of bR. The bR molecule contains a large number of weak acid residues, in particular aspartic with an apparent pK_a value as low as 3 or lower, where purple bR is transformed into blue,[1,57–62] and as high as 9.[34] At any given pH, one or more of these aspartic acids will have two forms, the neutral undissociated and the ionized negatively charged forms. It should be mentioned that there might be more than two types of bR, since different amino acids could be in different forms at any one pH. Depending on the time scale of the measurement, one can see one type or more.

Recently Jang and El-Sayed[63] showed that the fluorescence quenching probability of the different tryptophan molecules during the M_{412} in the bR photocycle is sensitive to pH with inflections at apparent pK_a values of 3, 5.5, and 9.5. This was explained in terms of protein conformation changes when one of the different amino acids with a pK_a value below 3 or around 5.5 and 9.5 changes its protonated state. Such protein conformation changes lead to changes in the relative orientation and/or distance between the different tryptophan residues and the retinal. This alters the probability of the energy transfer between different excited tryptophan molecules and retinal, thus changing the fluorescence quenching probability.

The above discussion and observations, as well as Raman spectroscopy[40] and pH and salt effects,[24,40,41,45,49] were explained in terms of protein heterogeneity as a cause for the observation of more than one rise and decay for the M_{412} intermediate. In general, there is no one-to-one correlation between the two components in the rise and that in the decay kinetics of the M_{412} intermediate. This might suggest that the pK_a of the acid (aspartic) that determines the heterogeneity changes upon M_{412} formation, i.e., upon the loss of the positive charge on the C=N nitrogen. This could lead to a change in the relative population of the ionized and nonionized forms of the acid creating the heterogeneity. If this occurs on a time scale that is not different from that for M decay, the correlation between the fast and slow amplitudes in the rise and decay of M will be lost. In the limit of having the equilibration time to be much faster than the M decay, one expects one decay component. Since at pH 7 the slow component is dominant and the population of the neutral form of the acid with pK_a near 9 is large, the slow component was assigned to the bR with the un-ionized form of the acid. If so, and since both components are comparable in the decay process, one concludes that the ionized form has increased when M_{412} is formed. Such a change in the environment within the active site must then lead to a decrease in the pK_a value of the acid that controls the relative amounts of the fast and slow components. One should emphasize that the bR species that has a fast rise does not have to have a fast decay and vice versa, since deprotonation and reprotonation represent different kinetic processes that are

(52) Oesterhelt, D.; Stoeckenius, W. *Methods Enzymol.* **1974**, *31*, 667.
(53) Becher, B. M.; Cassim, J. Y. *Prep. Biochem.* **1975**, *5*, 161.
(54) Herzfeld, J.; Das Gupta, S. K.; Farrar, M. R.; Harbison, G. S.; McDermott, A. E.; Pelletier, S. L.; Raleigh, D. P.; Smith, S. O.; Winkel, C.; Lugtenburg, J.; Griffin, R. G. *Biochemistry* **1990**, *29*, 5567.
(55) de Groot, H. J. M.; Smith, S. O.; Courtin, J.; van den Berg, E.; Windel, C.; Lugtenburg, J.; Griffin, R. G.; Herzfeld, J. *Biochemistry* **1990**, *29*, 6873.
(56) Maeda, A.; Ogura, T.; Kitigawa, T. *Biochemistry* **1986**, *25*, 2798.
(57) Moore, T. A.; Edgerton, M. E.; Parr, G.; Greenwood, C.; Perham, R. N. *Biochem. J.* **1978**, *171*, 469.
(58) Mowery, P. C.; Lozier, R. H.; Chae, Q.; Tseng, Y.-W.; Taylor, M.; Stocekenius, W. *Biochemistry* **1979**, *18*, 4100.
(59) Muccio, D. D.; Cassim, J. Y. *J. Mol. Biol.* **1979**, *135*, 595.
(60) Kimura, Y.; Ikegami, A.; Stoeckneius, W. *Photochem. Photobiol.* **1984**, *40*, 641.
(61) Fischer, U.; Oesterhelt, D. *Biophys. J.* **1979**, *28*, 211.
(62) Chronister, E. L.; Corcoran, T. C.; Songl, L.; El-Sayed, M. A. *Proc. Natl. Acad. Sci. U.S.A.* **1986**, *83*, 8530.
(63) Jang, D. J.; El-Sayed, M. A. *Proc. Natl. Acad. Sci. U.S.A.* **1989**, *86*, 5815.

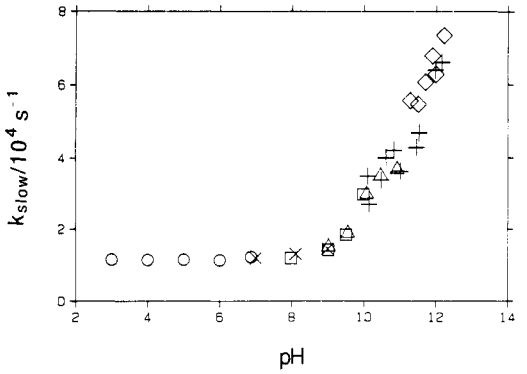

Figure 1. Dependence of rate constant k_{slow} on pH at room temperature ~22 °C. [Buffers used are indicated as follows: (○) KH_2PO_4; (×) Tris; (□) AMPSO; (△) AMP; (+) CAPS; (◇) K_2HPO_4.]

determined by the rate of change in the conformation of different portions of the protein.

From the above discussion we shall discuss our present results in terms of having two different types of bR, one with fast and one with slow formation rate for its M_{412}. The focus has been placed on the slow component.

2. Results and Possible Detailed Mechanism. The signal from the transient digitizer was found to fit closely to a biexponential form, corresponding to two parallel first-order reactions. The rate constants, k_{fast} and k_{slow}, and their associated relative amplitudes, C_{fast} and C_{slow}, were extracted by nonlinear least-squares fitting to

$$C(t) = C(\infty) - C_{fast}e^{-k_{fast}t} - C_{slow}e^{-k_{slow}t}$$

where

$$C_{fast} + C_{slow} = C(\infty) = 1$$

The pH profiles of the rate constant k_{slow} over the range pH 3–12 were obtained at temperature range 10–25 °C. A typical pH profile (at room temperature ~22 °C) is shown in Figure 1. Five overlapping buffer systems were used as shown by the different symbols in Figure 1. No significant specific effect of buffer species was observed.

The pH profile of the amplitude C_{slow} is given in Figure 3. The corresponding profile of C_{fast} is obtained simultaneously, since by definition $C_{fast} + C_{slow} = 1$. At pH 3–7, the reaction proceeds essentially 90% or more via the pathway of k_{slow}. At pH >8, C_{fast} increases at the expense of C_{slow}, tending to essentially 90% of the fast reaction pathway at pH 11. A plot of pR vs pH, where $R = C_{slow}/C_{fast}$, gives an apparent pK of 9.0 and $-\mathrm{dp}R/\mathrm{dpH} = n =$ 0.7–1 (see Appendix B). This implies that a single prototropic group with pK_a near 9 controls the population ratio of bR_{568} molecules which proceed along the fast or slow reaction pathway, in agreement with previous conclusions.[24] It is not clear what is happening to the amplitudes at pH >11. Apparently the slow pathway recovers, but we may possibly be observing a random coil conformer of L_{550}. The existence of a random coil conformer is surmised from the discontinuity observed in the pH profiles of the activation parameters, as discussed further below.

The Arrhenius energy E_a and the pre-exponential factor A were determined in the usual way by least-squares fitting to the equation $k = A\exp(-E_a/RT)$. At pH 3–7 the plots of ln k_{slow} vs $1/T$ are independent of pH as shown in Figure 2A, while in Figure 2B the Arrhenius plots at pH 8–12 show that while the slopes are not very sensitive to pH the value of the rate constant increases with pH, in agreement with previous results at room temperature.[24,42-44] The enthalpy of activation $\Delta H^{\ddagger}$ and the entropy of activation $\Delta S^{\ddagger}$ were calculated from the Arrhenius parameters by means of the following equations (see Appendix A):

$$\Delta H^{\ddagger} = E_a - 2.5\ \mathrm{kJ\ mol^{-1}} \qquad \text{at 25 °C}$$

$$\Delta S^{\ddagger} = R[\ln (A/\mathrm{s^{-1}}) - 30.5] \qquad \text{at 25 °C}$$

The values of ln (A/s^{-1}), E_a, $\Delta H^{\ddagger}$, and $\Delta S^{\ddagger}$ at pH 3–12 are given in Table I, and the pH profiles of $\Delta H^{\ddagger}$ and $\Delta S^{\ddagger}$ are shown in Figures 4 and 5, respectively.

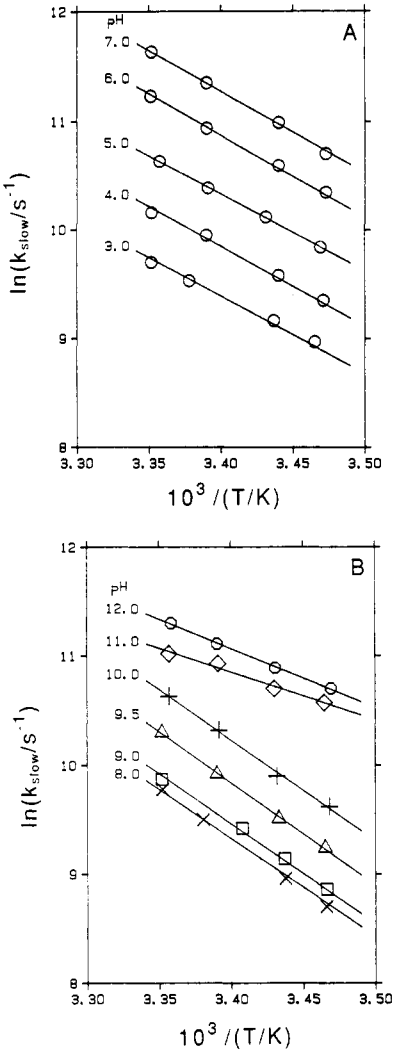

Figure 2. Arrhenius plots for k_{slow} at different pH values at ionic strength of ~0.11 M. In (A) the values are offset by increments of 0.5, 1.0, 1.5, and 2.0 for pH 4, 5, 6, and 7, respectively, in the ln (k_{slow}/s^{-1}) axis for clarity, since the Arrhenius plots in this pH range are virtually indistinguishable. There is no offset in (B).

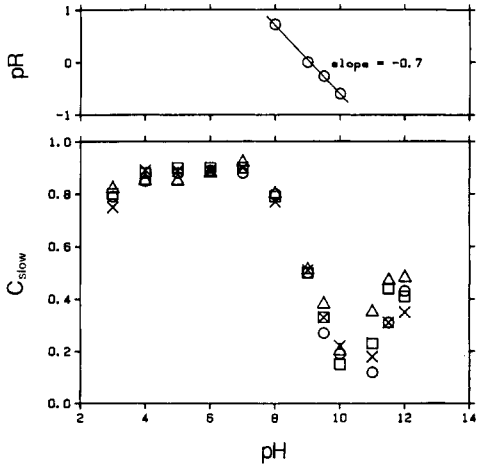

Figure 3. Dependence of the relative amplitude C_{slow} on pH. The corresponding value of C_{fast} can be obtained simultaneously since $C_{fast} + C_{slow} = 1$. Each symbol denotes the average value of C_{slow} obtained at a particular temperature [(○) ~25 °C; (×) ~22 °C; (□) ~18 °C; (△) ~15 °C]. The logarithm of the ratio $R = C_{slow}/C_{fast}$ in the pH range between 8 and 10 is also shown (see text for discussion).

The rate constant k_{slow} is remarkably independent of pH in the range pH 3–8. Above pH 8, the values of k_{slow} continue to increase

TABLE I: Dependence on pH of the Arrhenius Parameters of k_{slow} for the Deprotonation Step L → M

pH	ln (A/s^{-1})	E_a, kJ mol^{-1}	$\Delta H^{\ddagger}$, kJ mol^{-1}	$\Delta S^{\ddagger}$, J K^{-1} mol^{-1}
3.0	34	59	56	25
4.0	34	61	59	32
5.0	34	59	57	25
6.0	35	63	60	37
7.0	34	61	59	32
8.0	40	74	72	78
9.0	41	76	74	85
9.5	42	78	76	94
10.0	42	77	74	93
11.0	26	37	34	-39
12.0	30	45	43	-8

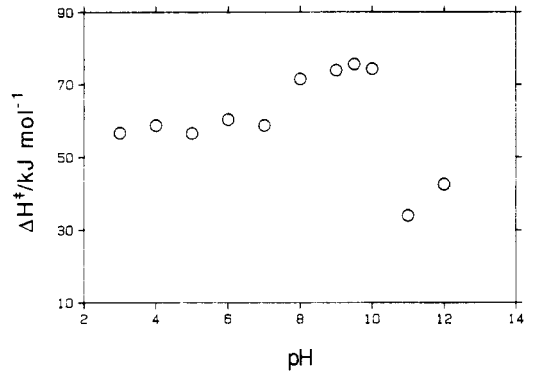

Figure 4. Dependence of the enthalpy of activation $\Delta H^{\ddagger}$ on pH.

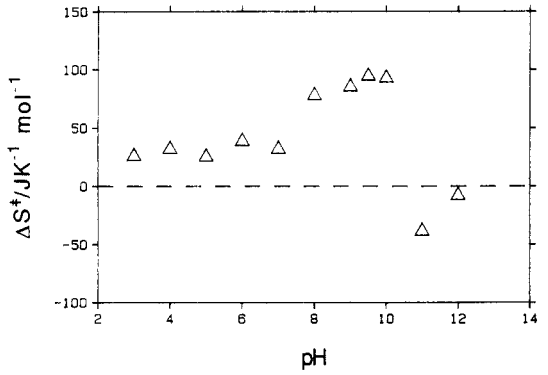

Figure 5. Dependence of the entropy of activation $\Delta S^{\ddagger}$ on pH.

apparently in a linear manner up to 8-fold at pH 12. There is no clear indication of a sigmoid dependence of k_{slow} on pH or of a plateau region, which could be linked to the pK_a of a discrete prototropic group. In contrast, the pH profiles of $\Delta H^{\ddagger}$ and $\Delta S^{\ddagger}$ both show sharp discontinuities at pH 10–11. Especially significant is the switch in the value of $\Delta S^{\ddagger}$ from a large positive value (+93 J K^{-1} mol^{-1} at pH 10) to a small negative value (-39 J K^{-1} mol^{-1} at pH 11 and -8.3 J K^{-1} mol^{-1} at pH 12).

At pH 3–7. There is practically no pH effect on k_{slow}, even though there must be a continuous buildup of negative charge on the protein with increasing pH due to nonspecific ionizations of many prototropic groups in proximity to the retinal and elsewhere. However, in this pH range both $\Delta H^{\ddagger}$ and $\Delta S^{\ddagger}$ increase with pH in a manner such that $\Delta H^{\ddagger} - T\Delta S^{\ddagger} = \Delta G^{\ddagger}$ is constant; that is to say, the enthalpy change is offset by the entropy change.

At pH 8–10. The buildup of negative surface charge becomes strong enough to affect k_{slow} in a manner which facilitates the deprotonation of the PSB as L_{550} changes into M_{412}, as is evident from the pronounced increase of k_{slow} with higher pH. In this pH range $T\Delta S^{\ddagger}$ increases more strongly than $\Delta H^{\ddagger}$; that is to say, $d\Delta G^{\ddagger}/dpH < 0$. The activation parameters are to be viewed in the light of the difference between the transition-state L‡ and the reactant L_{550} in the slow step of L → M. The increase in $\Delta H^{\ddagger}$ with higher pH means that larger activation enthalpies are needed to remove the proton from the PSB in a more negatively charged

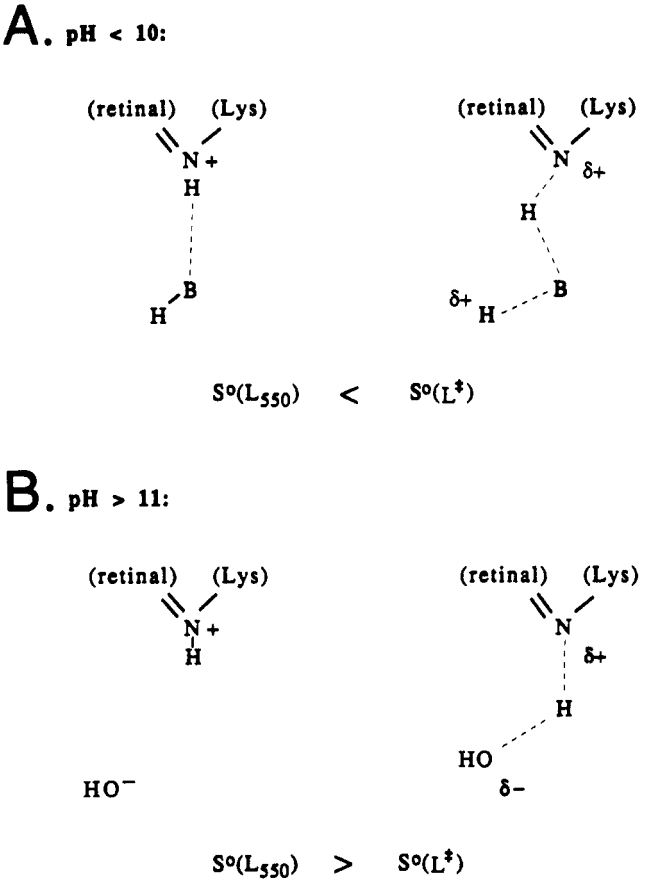

Figure 6. Models for the deprotonation mechanism: (A) at pH <10; (B) at pH >11.

local environment. The $\Delta S^{\ddagger}$ value relative to the reactant L_{550} shows more vigorous vibrational motion, more looseness of structure, and hence higher entropy. This can be understood to imply that in the reactant L_{550} there is considerable structural constraint, as would be the case if hydrogen bonding is involved between the PSB and one or more prototropic sites on the adjacent α-helices such as aspartate, as has been suggested in previous investigations[12,20] (see Figure 6A).

At pH 10–11. There is a transition which is reflected in the activation parameters but not seen in the value of k_{slow} itself. The transition is very abrupt. This is consistent with a cooperative hydroxide ion attack on the hydrogen bonding of the bR secondary structure, resulting in considerable loss of α-helix at least around the active site. If so, then the sharpness of the transition indicates a high reaction order in hydroxide

$$\text{helix} + n\text{OH}^- \rightleftharpoons \text{random coil}$$

at equilibrium

$$K_{OH} = [\text{coil}]/[\text{helix}][\text{OH}^-]^n = R([\text{H}^+]/K_w)^n$$

or

$$K_H = (K_w)^n K_{OH} = R[\text{H}^+]^n$$

where R = [coil]/[helix] and the ion product of water K_w = [H$^+$][OH$^-$]. Hence

$$pR = pK_H - n\text{pH}$$

A plot of pR vs pH should give $-dpR/dpH = n$ (see Appendix B). A value of $n = 4$ is consistent with the kinetic data and an apparent average pK_a = pK_H/4 = 10.5. This equilibrium implies that in the range pH 10–11 we encounter the transition between L_{550} (helical) and L_{550} (nonhelical). A similar simultaneous multiproton equilibrium was reported by Awad and Badro,[64] who

(64) Awad, E. S.; Badro, R. G. *Biochemistry* **1967**, *6*, 1785.

observed a value of $n = 5$ in the pH-dependent kinetics of the sperm whale ferrimyoglobin reaction with cyanide ion. On the basis of the values found for pK_a, $\Delta H°$, and $\Delta S°$, it was suggested that the simultaneous ionization of five carboxyl groups controlled the pH-dependent transition between two reacting conformers of sperm whale ferrimyoglobin.

At pH 11–12. To account for the change in the sign of $\Delta S^‡$, we propose that the deprotonation of the PSB proceeds by transference of H^+ directly to a hydroxide ion or water solvent, since in the random coil conformation of the PSB environment there will be easy access of the external aqueous phase to the deprotonation site. Now the entropy in the transition-state $L^‡$ will be lower than in the reactant L_{550}, because the structuring that existed in the helical conformer, such as hydrogen bonding, would be absent in the nonhelical conformer and there will be, to a small extent, new structuring in the transition-state $L^‡$ (nonhelical) due to association of the PSB with OH^- or H_2O (see Figure 6B). The involvement of H_2O in the reaction mechanism is relevant by virtue of the great preponderance of H_2O in the medium compared to OH^-. The following representations are effectively the same:

$$\sim HN^+ + OH^- \rightarrow \sim N: + HOH \quad (1)$$

$$\sim NH^+ + HOH \rightarrow \sim N: + H_3O^+ \quad (2)$$

$$H_3O^+ + OH^- \rightarrow 2H_2O$$

Alternatively, a prototropic group on the random coil approaching the PSB would result in some limited structuring in the transition state, so that $S°(L_{550}) > S°(L^‡)$, and hence $\Delta S^‡ < 0$. The sudden decrease in the activation energy of the deprotonation process in this pH range (~40 kJ/mol as compared to 70 kJ/mol for pH 10 and lower) strongly suggests that, in this open structure, this process is changing toward a "restricted" diffusion-controlled limit. This could suggest that the rate of the deprotonation process is limited by the rate by which H_2O (or OH^-) reaches the vicinity of the PSB. Of course this diffusion seems to have a higher barrier in the protein as compared to that in H_2O, since the latter has an activation energy of only 13 kJ/mol.

The large decrease in the activation energy and the accompanying change in the sign of the entropy change are observed in the reprotonation process of some mutants, e.g., Asp-96 → Asn, Asp → Gly,[65] and Arg-227 → Gln.[66] In these cases, the mutation must have opened the structure of the protein in such a manner to make the process of reprotonation (restricted) diffusion controlled.

Acknowledgment. This work was supported by the Department of Energy under Grant DE-FG03-88ER13828. The computer program for the data analysis and the interface for the new system were set up by Hyun-Jin Hwang and Yue-Jin Chang.

Appendix A

The rate constant according to Arrhenius is given by the equation

$$k = Ae^{-E_a/RT}$$

where the Arrhenius energy, E_a, and the pre-exponential factor, A, are assumed to be independent of T. According to Wynne-Jones and Eyring[67]

$$k = (\mathbf{k}T/\mathbf{h}) \exp(-\Delta G^‡/RT)$$

$$\Delta G^‡ = \Delta H^‡ - T\Delta S^‡$$

assuming $\Delta H^‡$ and $\Delta S^‡$ to be independent of T. Subject to these assumptions and using straightforward algebraic manipulation:

$$\ln k = \ln A - E_a/RT = \ln (\mathbf{k}/\mathbf{h}) - \ln (1/T) + \Delta S^‡/R = \Delta H^‡/RT$$

$$[\partial \ln k/\partial(1/T)]_p = -E_a/R = -T - \Delta H^‡/R$$

Hence

$$\Delta H^‡ = E_a - RT = E_a - 2.5 \text{ kJ mol}^{-1} \quad \text{at } 25°C$$

and

$$\Delta S^‡/R = \ln (A\mathbf{h}/\mathbf{k}T) - 1 = \ln (A/\text{s}^{-1}) - 30.5 \quad \text{at } 25 °C$$

Appendix B

Consider the prototropic equilibrium

$$P(GH)_n \rightleftharpoons P(G^-)_n + nH^+$$

where P represents a protein molecule and GH an acidic amino acid residue. We may write more simply

$$A \rightleftharpoons B + nH^+$$

where the equilibrium constant is given by

$$K = (B)(H^+)^n/(A)$$

Putting

$$R = (B)/(A)$$

we have

$$pR = pK_n - n\text{pH}$$

The prototropic equilibrium for an individual group GH is given by

$$GH \rightleftharpoons G^- + H^+$$

with

$$K_a = (G^-)(H^+)/(GH)$$

For noninteracting sites, $(G^-)/(GH) = P(G^-)_n/P(GH)_n = R$, hence

$$pR = pK_a - \text{pH}$$

When $R = 1$, $pR = 0$ and $pK = npK_a$. The ratio of concentrations, R, is obtained experimentally by measurement of some parameter which is associated with species A or with species B. An analysis similar to the preceding was given by Awad and Badro.[64]

Registry No. H^+, 12408-02-5.

(65) Miller, A.; Oesterhelt, D. *Biochim. Biophys. Acta* **1990**, *1020*, 57.
(66) Lin, G. C.; El-Sayed, M. A.; Stern, L. J.; Marti, T.; Mogi, T.; Khorana, H. G. *Biophys. J.* 1991, in press.
(67) Wynne-Jones, W. F. K.; Eyring, H. *J. Chem. Phys.* **1935**, *3*, 492.